

Locally Optimal Preconditioned Conjugate Gradient Method for Computing Ground State of Space-Fractional Nonlinear Schrödinger Equation

Biyun Zhu, Aiguo Xiao and Xueyang Li*

School of Mathematics and Computational Science, Hunan Key Laboratory for Computation and Simulation in Science and Engineering, Key Laboratory of Intelligent Computing and Information Processing of Ministry of Education, Xiangtan University, Xiangtan 411105, P.R. China

Received 8 September 2025; Accepted (in revised version) 18 December 2025

Abstract. In this paper, we investigate numerical methods for computing the ground state of space-fractional nonlinear Schrödinger equation. We focus on extending the locally optimal preconditioned conjugate gradient method, originally designed for linear eigenvalue problems, to address this nonlinear fractional framework. Through comparative numerical experiments with the discrete gradient flow method, we demonstrate that the locally optimal preconditioned conjugate gradient method achieves significantly superior efficiency in many scenarios. This advantage is particularly pronounced in multidimensional problems and cases involving lower fractional derivative orders. The results highlight the adaptability of the locally optimal preconditioned conjugate gradient approach to eigenproblem of fractional nonlinear systems, offering a robust and high efficient computational alternative for high-dimensional or low-order fractional derivative settings.

AMS subject classifications: 35R11, 65H17, 65T40, 81-08

Key words: Nonlinear Schrödinger equation, fractional Laplacian, ground state, sine pseudo-spectral method, locally optimal preconditioned conjugate gradient method.

1. Introduction

Consider the time-dependent space-fractional nonlinear Schrödinger equation

$$i \frac{\partial \psi}{\partial t} = \frac{1}{2} (-\Delta)^{\frac{\alpha}{2}} \psi + V(\mathbf{x})\psi + f(|\psi|^2)\psi, \quad \mathbf{x} \in \Omega \subset \mathbb{R}^d, \quad t > 0, \quad (1.1)$$

where $\psi = \psi(\mathbf{x}, t)$ is a complex-valued wave function, $V(\mathbf{x})$ denotes an external poten-

*Corresponding author. *Email address:* lixy1217@xtu.edu.cn (X. Li)

tial function, and the nonlinear term $f(\cdot)$ represents the interaction potential. In this paper, we focus on the problem of bound state. For bound state, the distribution of wave functions will be highly concentrated within a finite region, and many physical models approximately assume that the external potential $V(\mathbf{x})$ takes a positive infinite value outside of the finite region. Therefore, the original problem can be approximately transformed into the problem of homogeneous Dirichlet boundary conditions [7], i.e. let

$$\Omega = (0, R)^d$$

be a finite region with some positive real number R , and

$$\psi(\mathbf{x}, t) = 0, \quad \mathbf{x} \in \partial\Omega, \quad t \geq 0.$$

Moreover, we assume that the value of $V(\mathbf{x})$ at the boundary of Ω is significantly greater than the value at the middle of Ω . Under this assumption, the wave function can be expressed as a linear combination of sine basis functions, i.e.

$$\psi(\mathbf{x}, t) = \sum_{\mathbf{k} \in \mathbb{N}_+^d} \hat{\psi}_{\mathbf{k}} \varphi_{\mathbf{k}}(\mathbf{x}),$$

where \mathbb{N}_+ denotes the set of positive integers, and the basis functions are chosen as

$$\varphi_{\mathbf{k}}(\mathbf{x}) = \prod_{j=1}^d \sin\left(\frac{k_j \pi x_j}{R}\right).$$

$(-\Delta)^{\alpha/2}$ denotes the fractional Laplace operator, which is defined as follows [24]:

$$(-\Delta)^{\frac{\alpha}{2}} \psi(\mathbf{x}, t) = \frac{\pi^\alpha}{R^\alpha} \sum_{\mathbf{k} \in \mathbb{N}_+^d} \|\mathbf{k}\|^\alpha \hat{\psi}_{\mathbf{k}}(t) \varphi_{\mathbf{k}}(\mathbf{x}), \quad (1.2)$$

where

$$\|\mathbf{k}\| = (k_1^2 + k_2^2 + \cdots + k_d^2)^{\frac{1}{2}}.$$

The sine coefficients are defined as

$$\hat{\psi}_{\mathbf{k}}(t) = \frac{2^d}{R^d} \int_{\Omega} \psi(\mathbf{x}) \varphi_{\mathbf{k}}(\mathbf{x}) d\mathbf{x}, \quad \mathbf{k} \in \mathbb{N}_+^d. \quad (1.3)$$

Eq. (1.1) possesses two conserved quantities, namely mass conservation (unitarity)

$$\|\psi(\cdot, t)\|^2 = \int_{\Omega} |\psi(\mathbf{x}, t)|^2 d\mathbf{x} \equiv 1, \quad (1.4)$$

and energy conservation $E(\psi(\cdot, t)) \equiv C$, where the energy functional is defined as

$$E(u) = \int_{\Omega} \left(\frac{1}{2} \overline{u(\mathbf{x})} (-\Delta)^{\frac{\alpha}{2}} u(\mathbf{x}) + V(\mathbf{x}) |u(\mathbf{x})|^2 + F(|u(\mathbf{x})|^2) \right) d\mathbf{x}, \quad (1.5)$$

where

$$F(s) = \int_0^s f(\tau) d\tau.$$

Many physics studies are more concerned with stationary problems in quantum mechanics. In stationary problems, the wave function can be expressed as the product of a time-independent function and a phase factor, i.e.

$$\psi(\mathbf{x}, t) = e^{-i\lambda t} u(\mathbf{x}).$$

Thus, the nonlinear stationary Schrödinger equation is

$$\begin{aligned} \lambda u(\mathbf{x}) &= \frac{1}{2}(-\Delta)^{\frac{\alpha}{2}} u(\mathbf{x}) + V(\mathbf{x})u(\mathbf{x}) + f(|u(\mathbf{x})|^2)u(\mathbf{x}), \quad \mathbf{x} \in \Omega, \\ u(\mathbf{x}) &= 0, \quad \mathbf{x} \in \partial\Omega, \\ \|u\|^2 &= 1. \end{aligned} \tag{1.6}$$

The above equation is also referred to as the eigenvalue problem for the nonlinear Schrödinger operator, where λ is termed the eigenvalue of the nonlinear Schrödinger operator and $u(\mathbf{x})$ is termed the corresponding eigenfunction. Furthermore, $\|u\|^2 = 1$ corresponds to the mass conservation (1.4) in the time-dependent problem, thus serving as a mass constraint or normalization condition for the eigenvalue problem. Solutions to the eigenvalue problem (1.6) are generally non-unique. Typically, the energy possesses a minimum value, and the eigenfunction corresponding to this minimal energy is defined as the ground state

$$u_g = \operatorname{argmin}_{u \in \mathcal{S}} E(u), \quad \mathcal{S} := \{u : \|u\|^2 = 1, E(u) < +\infty\}. \tag{1.7}$$

Consequently, the ground state represents the most prevalent and stable quantum state. All eigenfunctions $u(\mathbf{x})$ satisfy the stationary equation (1.6), except for the ground state, are called excited states. In this paper, we only research the numerical solution for ground state.

The space-fractional Schrödinger equation was derived by Laskin through Lévy path integrals [18, 19]. In space-fractional nonlinear Schrödinger equation, the fractional-order α directly governs wave packet propagation: as α decreases from 2 (the classical limit), wave packets exhibit slower spatial dispersion and altered interference patterns, enabling phenomena like self-decelerating Airy beams and modified quantum tunneling. And it has widely application in the field of spanning optical trapping [23], condensed matter physics [10], diffraction-free beams [32], and so on.

In recent years, there have been many numerical methods studies on the time-dependent space-fractional Schrödinger equation. Wang *et al.* [27] constructed a linear implicit conservative difference scheme for solving the coupled fractional nonlinear Schrödinger equation. Li *et al.* [20] proposed using the finite element method to solve the strongly coupled nonlinear fractional Schrödinger equation. Liang *et al.* [21] discussed the Fourier spectral exponential time difference method for the spatial fractional

nonlinear Schrödinger equation. Other numerical methods for the spatial fractional Schrödinger equation can be found in [13, 25, 28, 33] and their references.

An important studies of this paper is the numerical iterative methods for solving the ground state. For this problem, the most commonly used method is the discrete gradient flow method. The idea of this method is to transform the minimum energy problem into a time-dependent problem for computation, and to maintain the mass constraint through normalization corrections. Bao *et al.* [3–5] and Cai *et al.* [8] have conducted extensive research on the discrete gradient flow method. For the fractional-order case, Chang [9] and Liu *et al.* [22] studied the ground state of the fractional Schrödinger equation using the variational method. Duo *et al.* [12] applied the discrete gradient flow method to study the fractional Schrödinger equation in an infinite potential well. Yang *et al.* [31] proved the energy diminishing estimate of the discrete gradient flow method for solving the fractional stationary Schrödinger equation.

Besides, other iterative methods have also been used to compute the ground state, such as the conjugate gradient method [2], Newton-Noda iteration method [11], and so on. However, as far as we know, these methods have not been considered for fractional-derivative case. The preconditioned conjugate gradient method was originally developed to solve large linear systems of equations, primarily for symmetric positive-definite matrices. Subsequently, some researchers applied the preconditioned conjugate gradient method to solving eigenvalue problems [16, 30]. However, some of the favorable properties of the preconditioned conjugate gradient method when solving linear algebraic equations (such as the conjugate orthogonality of all search directions) are not inherited when solving eigenvalue problems. This makes it difficult to directly determine the optimal search direction in each iteration. Although the preconditioned conjugate gradient method is primarily used for solving linear problems, it can also be applied to handle certain weakly nonlinear problems. By utilizing the results of the previous iteration, the nonlinear operator can be approximately treated as a linear operator, and then the preconditioned conjugate gradient method can be used for iterative computation in that step. In [2], the preconditioned conjugate gradient method has been used in computing the nonlinear ground state for integer-order case.

The locally optimal preconditioned conjugate gradient method and locally optimal preconditioned conjugate gradient (LOBPCG) method were proposed by Knyazev [17] in 2001, and they are improved versions of the preconditioned conjugate gradient method used for solving eigenvalue problems. Benner *et al.* [6] estimated the convergence of this method. For nonlinear problems, since the temporary linear operator is not fixed, the block preconditioned conjugate gradient technique cannot be used. Therefore, this paper only considers the locally optimal preconditioned conjugate gradient method. In each iteration, the locally optimal preconditioned conjugate gradient method selects the optimal search direction through a local optimization strategy, whereas the preconditioned conjugate gradient method only relies on the standard orthogonalization step. As a result, the locally optimal preconditioned conjugate gradient method can better control the iteration direction, accelerating convergence and avoiding the oscillations or slow convergence that may occur in the preconditioned conjugate

gradient method. Although it increases the number of times the linear operator needs to be computed in each iteration, this additional cost is worthwhile overall.

The remainder of this paper is systematically organized as follows. In Section 2, we use the sine pseudospectral method to provide the spatial discretization scheme of the space-fractional nonlinear Schrödinger equation (1.6). In Section 3, we briefly introduce the algorithm process of the discrete gradient flow method. In Section 4, by setting the provisional linear operators in the iteration steps, we promote the locally optimal preconditioned conjugate gradient method to compute the ground state of fractional-order nonlinear problem. In Section 5, numerical experiments are carried out to verify the efficiency of locally optimal preconditioned conjugate gradient method. In Section 6, we have summarized the advantages and prospects of locally optimal preconditioned conjugate gradient method in computing the stationary solution of space-fractional nonlinear Schrödinger equation.

2. Sine pseudospectral method

For the nonlinear eigenvalue problem (1.6), spatial discretization is first performed using the sine pseudo-spectral method. For a given positive integer K , define the set of coefficient indices

$$\mathcal{K} = \{1, 2, \dots, K-1\}^d, \quad (2.1)$$

grid points

$$\mathcal{G} = \left\{ \frac{R}{K} \mathbf{k} : \mathbf{k} \in \mathcal{K} \right\}, \quad (2.2)$$

and function space

$$\mathcal{U} = \text{span}\{\varphi_{\mathbf{k}}\}_{\mathbf{k} \in \mathcal{K}}. \quad (2.3)$$

Consequently, the interpolation operator can be defined as

$$\begin{aligned} \mathcal{I} : C_0(\Omega) &\rightarrow \mathcal{U} \\ : u(\mathbf{x}) &\mapsto \mathcal{I}u(\mathbf{x}) = \sum_{\mathbf{k} \in \mathcal{K}} \tilde{u}_{\mathbf{k}} \varphi_{\mathbf{k}}(\mathbf{x}), \end{aligned} \quad (2.4)$$

where the discrete sine coefficients $\tilde{u}_{\mathbf{k}}$, $\mathbf{k} \in \mathcal{K}$ are given by

$$(\tilde{u}_{\mathbf{k}})_{\mathbf{k} \in \mathcal{K}} = \mathbf{S}(u(\boldsymbol{\xi}))_{\boldsymbol{\xi} \in \mathcal{G}} = \left(\frac{2^d}{K^d} \sum_{\boldsymbol{\xi} \in \mathcal{G}} u(\boldsymbol{\xi}) \varphi_{\mathbf{k}}(\boldsymbol{\xi}) \right)_{\mathbf{k} \in \mathcal{K}}. \quad (2.5)$$

The matrix \mathbf{S} here is a mapping from the grid function $(u(\boldsymbol{\xi}))_{\boldsymbol{\xi} \in \mathcal{G}}$ to the coefficient vector $(\tilde{u}_{\mathbf{k}})_{\mathbf{k} \in \mathcal{K}}$, which is called the discrete sine transform. This transform can be efficiently computed using the fast Fourier transform (FFT), and its asymptotic time complexity is of order $\mathcal{O}(K^d \log K)$. Regarding the matrix \mathbf{S} , it can be readily shown that it is symmetric and invertible, satisfying $\mathbf{S} = (2^d/K^d)\mathbf{S}^{-1}$. Consequently, the

stationary problem (1.6) discretized via the sine pseudo-spectral method reduces to finding eigenpairs $(\lambda, U) \in \mathbb{R} \times (\mathcal{U} \cap \mathcal{S})$ such that

$$\lambda U(\mathbf{x}) = \frac{1}{2}(-\Delta)^\alpha U(\mathbf{x}) + \mathcal{I}(V(\mathbf{x})U(\mathbf{x})) + \mathcal{I}(f(|U(\mathbf{x})|^2)U(\mathbf{x})). \quad (2.6)$$

Let

$$\hat{\mathbf{U}} = (\hat{U}_{\mathbf{k}})_{\mathbf{k} \in \mathcal{K}}, \quad \mathbf{U} = \mathbf{S}^{-1}\hat{\mathbf{U}} = (U(\boldsymbol{\xi}))_{\boldsymbol{\xi} \in \mathcal{G}}.$$

The discrete scheme in (2.6) can be expressed in the following vector form:

$$\lambda \hat{\mathbf{U}} = \mathbf{H}(\mathbf{U})\hat{\mathbf{U}} = \boldsymbol{\Lambda}\hat{\mathbf{U}} + \mathbf{S}\mathbf{V}\mathbf{S}^{-1}\hat{\mathbf{U}} + \mathbf{S}\mathbf{f}(\mathbf{U})\mathbf{S}^{-1}\hat{\mathbf{U}}, \quad (2.7)$$

where

$$\boldsymbol{\Lambda} = \text{diag} \left(\frac{\pi^\alpha \|\mathbf{k}\|^\alpha}{2R^\alpha} \right)_{\mathbf{k} \in \mathcal{K}}, \quad \mathbf{V} = \text{diag}(V(\boldsymbol{\xi}))_{\boldsymbol{\xi} \in \mathcal{G}}, \quad \mathbf{f}(\mathbf{U}) = \text{diag}(f(|U(\boldsymbol{\xi})|^2))_{\boldsymbol{\xi} \in \mathcal{G}}.$$

For the coefficient vectors $\hat{\mathbf{U}}, \hat{\mathbf{W}} \in \mathbb{R}^{\mathcal{K}}$, we can define a discrete inner product

$$\langle \hat{\mathbf{U}}, \hat{\mathbf{W}} \rangle = \frac{R^d}{2^d} \sum_{\mathbf{k} \in \mathcal{K}} \hat{U}_{\mathbf{k}} \hat{W}_{\mathbf{k}}.$$

Then, the discrete form of the normalization condition can be expressed as

$$\|\hat{\mathbf{U}}\|^2 = \langle \hat{\mathbf{U}}, \hat{\mathbf{U}} \rangle = 1. \quad (2.8)$$

Therefore, once the numerical solution $U \in \mathcal{U}$ is obtained, the energy in (1.5) can be approximated via the following scheme:

$$E(U) \approx E_K(\hat{\mathbf{U}}) = \langle \hat{\mathbf{U}}, \boldsymbol{\Lambda}\hat{\mathbf{U}} + \mathbf{S}\mathbf{V}\mathbf{S}^{-1}\hat{\mathbf{U}} \rangle + \frac{R^d}{K^d} \sum_{\boldsymbol{\xi} \in \mathcal{G}} F(|U(\boldsymbol{\xi})|^2). \quad (2.9)$$

Next, we will discuss the numerical iterative method for finding the minimum value of the discrete energy functional (2.9).

3. Discrete gradient flow method

The discrete gradient flow method is a conventional approach for computing fractional-order nonlinear ground states, and it has been researched in [12, 31]. In this section, we introduce the discrete gradient flow method as a reference standard numerical method to provide a comparison for the locally optimal preconditioned conjugate gradient method. The goal of the gradient flow method is to find the minimum value of the energy functional $E(u)$ defined by Eq. (1.5) under the normalization condition $\|u\| = 1$. In this method, u is first treated as a state function with the variable t , and an initial function $u(\mathbf{x}, 0) = u_0(\mathbf{x})$ is chosen somewhat arbitrarily. Then, $u(\mathbf{x}, t)$ evolves in

the direction of the negative gradient of the energy functional $E(u)$ to achieve a lower energy value. Since changes along the negative gradient direction will disrupt the normalization condition, the wave function must be renormalized after each time step. This leads to the following gradient flow method with normalization:

$$\begin{aligned} \frac{\partial}{\partial t} u &= -\frac{1}{2} \frac{\delta E(u)}{\delta u} = -\frac{1}{2} (-\Delta)^\alpha u - V(\mathbf{x})u - f(|u|^2)u, \quad t_n < t < t_{n+1}, \\ u(\mathbf{x}, t_{n+1}) &= \frac{u(\mathbf{x}, t_{n+1}^-)}{\|u(\cdot, t_{n+1}^-)\|}, \\ u(\mathbf{x}) &= 0, \quad \mathbf{x} \in \partial\Omega, \\ u(\mathbf{x}, 0) &= u_0(\mathbf{x}), \end{aligned} \quad (3.1)$$

where $n \geq 0$, the time sequence satisfies $0 = t_0 < t_1 < t_2 < \dots < t_n < \dots$, and $u(\cdot, t_{n+1}^-)$ denotes the left limit in the temporal direction $\lim_{t \rightarrow t_{n+1}^-} u(\cdot, t)$. Similar to the numerical scheme in Eq. (2.7), the sine pseudospectral method is used for spatial discretization of Eq. (3.1). Thus, it follows that

$$\begin{aligned} \hat{\mathbf{U}}'(t) &= -\mathbf{H}(\mathbf{U}(t))\hat{\mathbf{U}}(t), \quad t_n < t < t_{n+1}, \\ \hat{\mathbf{U}}(t_{n+1}) &= \frac{\hat{\mathbf{U}}(t_{n+1}^-)}{\|\hat{\mathbf{U}}(t_{n+1}^-)\|}, \\ \hat{\mathbf{U}}(0) &= \hat{\mathbf{U}}_0. \end{aligned} \quad (3.2)$$

Then, the backward Euler method is generally adopted for temporal discretization of (3.2), yielding the following fully discrete scheme:

$$\begin{aligned} \frac{\hat{\mathbf{U}}_{n+1,-} - \hat{\mathbf{U}}_n}{\Delta t} &= -\mathbf{H}(\mathbf{U}_n)\hat{\mathbf{U}}_{n+1,-}, \\ \hat{\mathbf{U}}_{n+1} &= \frac{\hat{\mathbf{U}}_{n+1,-}}{\|\hat{\mathbf{U}}_{n+1,-}\|}, \quad \lambda_{n+1} = \frac{1 - \|\hat{\mathbf{U}}_{n+1,-}\|}{\Delta t \|\hat{\mathbf{U}}_{n+1,-}\|}, \end{aligned} \quad (3.3)$$

where $\Delta t = t_{n+1} - t_n$ for $n = 0, 1, \dots$. The termination condition of iteration (3.3) is

$$\frac{\|\mathbf{H}(\mathbf{U}_n)\hat{\mathbf{U}}_n - \lambda_n \hat{\mathbf{U}}_n\|}{\max\{1, |\lambda_n|\}} < \epsilon,$$

where ϵ is a given threshold. It is worth noting that the scheme in (3.3) is a linear implicit scheme rather than a nonlinear implicit scheme, meaning that the fully discretized scheme requires solving a system of linear algebraic equations. This system of linear equations can be solved by using the following simple iterative method:

$$\left(\frac{1}{\Delta t} \mathbf{I} + \mathbf{\Lambda} + a_{\text{opt}} \mathbf{I} \right) \hat{\mathbf{U}}_{n+1}^{(p+1)} = (a_{\text{opt}} \mathbf{I} - \mathbf{S} \mathbf{V} \mathbf{S}^{-1} - \mathbf{S} \mathbf{f}(\mathbf{U}_n) \mathbf{S}^{-1}) \hat{\mathbf{U}}_{n+1}^{(p)} + \frac{1}{\Delta t} \hat{\mathbf{U}}_n \quad (3.4)$$

for $p \geq 0$ and $\hat{\mathbf{U}}_{n+1}^{(0)} = \hat{\mathbf{U}}_n$, where the optimization factor is obtained by

$$a_{\text{opt}} = \frac{1}{2} \left(\max_{\boldsymbol{\xi} \in \mathcal{G}} (V(\boldsymbol{\xi}) + f(|U(\boldsymbol{\xi})|^2)) + \min_{\boldsymbol{\xi} \in \mathcal{G}} (V(\boldsymbol{\xi}) + f(|U(\boldsymbol{\xi})|^2)) \right).$$

The computational performance of the discrete gradient flow method (3.3) depends on the time step size Δt . If Δt is too small, it restricts the search scope per step, leading to slower convergence of iterations. If Δt is too large, it may cause the linear system (3.4) to become ill conditioned and difficult to compute. In summary, although the discrete gradient flow method demonstrates robust convergence properties, its computational efficiency still has room for improvement.

4. Locally optimal preconditioned conjugate gradient method

This section will focus on applying the locally optimal preconditioned conjugate gradient method to compute solutions for the discrete nonlinear eigenvalue problem (2.7).

Suppose $(\lambda_n, \hat{\mathbf{U}}_n)$ is a provisional eigenpair obtained at the n -th iteration step for the nonlinear eigenvalue problem (2.7). Using $\mathbf{U}_n = \mathbf{S}^{-1} \hat{\mathbf{U}}_n$, we obtain the required provisional linear operator $\mathbf{H}(\mathbf{U}_n)$ for the n -th computation step. The original problem thus reduces to solving the following linear eigenvalue problem for the eigenpair $(\lambda_{n+1}, \mathbf{U}_{n+1})$ as

$$\lambda_* \hat{\mathbf{U}}_* = \mathbf{H}(\mathbf{U}_n) \hat{\mathbf{U}}_*.$$

The above problem is equivalent to solving

$$\hat{\mathbf{U}}_* = \underset{\hat{\mathbf{U}} \in \mathbb{R}^{\mathcal{K}} \setminus \{\mathbf{0}\}}{\operatorname{argmin}} \frac{\langle \hat{\mathbf{U}}, \mathbf{H}(\mathbf{U}_n) \hat{\mathbf{U}} \rangle}{\langle \hat{\mathbf{U}}, \hat{\mathbf{U}} \rangle}.$$

The conjugate gradient method falls under the category of Rayleigh-Ritz projection methods, whose fundamental concept involves projecting the original problem onto a low-dimensional subspace for solution. Suppose that $\mathbf{w}_n^{(1)}, \mathbf{w}_n^{(2)}, \dots, \mathbf{w}_n^{(m)} \in \mathbb{R}^{\mathcal{K}}$ are linearly independent vectors obtained at the n -th iteration, and let

$$\mathbf{W}_n = \left[\mathbf{w}_n^{(1)}, \mathbf{w}_n^{(2)}, \dots, \mathbf{w}_n^{(m)} \right].$$

The problem to be solved at this stage is

$$\mathbf{y}_n = \underset{\mathbf{y} \in \mathbb{R}^m \setminus \{\mathbf{0}\}}{\operatorname{argmin}} \frac{\langle \mathbf{W}_n \mathbf{y}, \mathbf{H}(\mathbf{U}_n) \mathbf{W}_n \mathbf{y} \rangle}{\langle \mathbf{W}_n \mathbf{y}, \mathbf{W}_n \mathbf{y} \rangle}.$$

Thus, a generalized eigenvalue problem for an m -dimensional vector is obtained as

$$\mu (\mathbf{W}_n)^T \mathbf{W}_n \mathbf{y} = (\mathbf{W}_n)^T \mathbf{H}(\mathbf{U}_n) \mathbf{W}_n \mathbf{y}.$$

Here, m is usually chosen as a number that is not very large. This implies that the aforementioned expression is a low-dimensional eigenvalue problem. Therefore, all

elements of the matrices $(\mathbf{W}_n)^T \mathbf{W}_n$ and $(\mathbf{W}_n)^T \mathbf{H}(\mathbf{U}_n) \mathbf{W}_n$ can be explicitly provided, and some numerical methods suitable for low-dimensional problems (such as the QR algorithm) can be employed for computation. Thus, the key to the Rayleigh-Ritz projection method lies in selecting appropriate vectors $\mathbf{w}_n^{(1)}, \mathbf{w}_n^{(2)}, \dots, \mathbf{w}_n^{(m)} \in \mathbb{R}^{\mathcal{K}}$.

The locally optimal preconditioned conjugate gradient method employs the Rayleigh-Ritz projection with $m = 3$. Within this framework, $\mathbf{w}_n^{(1)}$ and $\mathbf{w}_n^{(2)}$ are selected as $\hat{\mathbf{U}}_n$ (obtained from the n -th step of the locally optimal preconditioned conjugate gradient iteration) and the search direction \mathbf{p}_n , respectively. The remaining vector $\mathbf{w}_n^{(3)}$ needs to be computed in the $(n + 1)$ -th step. First, the following residual needs to be calculated:

$$\mathbf{r}_n = \mathbf{H}(\mathbf{U}_n) \hat{\mathbf{U}}_n - \lambda_n \hat{\mathbf{U}}_n.$$

It is noteworthy that the linear operator $\mathbf{H}(\mathbf{U}_n)$ is often ill-conditioned. Therefore, it is necessary to introduce a preconditioner \mathbf{P}_n . This preconditioner must be positive definite, computationally inexpensive, and capable of significantly reducing the condition number of the matrix $\mathbf{P}_n \mathbf{H}(\mathbf{U}_n)$. This paper employs a preconditioner with a diagonal matrix structure, described as follows:

$$\mathbf{P}_n = \left[\text{diag} \left(\max \left\{ 1, \left| \lambda_n + \frac{\pi^\alpha \|\mathbf{k}\|^\alpha}{2R^\alpha} \right| \right\} \right)_{\mathbf{k} \in \mathcal{K}} \right]^{-1}. \quad (4.1)$$

Therefore, $\mathbf{w}_n^{(3)}$ is chosen as the preconditioned residual, namely $\mathbf{w}_n^{(3)} = \mathbf{P}_n \mathbf{r}_n$. The complete algorithmic procedure for the locally optimal preconditioned conjugate gradient method to compute the nonlinear eigenvalue problem (2.7) is summarized in Algorithm 4.1.

Algorithm 4.1 The Minimum Eigenvalue Problem of (2.7) is Solved Using the Locally Optimal Preconditioned Conjugate Gradient Method

- 1: Select an iteration threshold ϵ , an initial search direction $\mathbf{p}_0 = \mathbf{0}$, and a starting vector $\hat{\mathbf{U}}_0$ satisfying the normalization condition (2.8).
- 2: **for** $n = 0, 1, 2, \dots$, **do**
- 3: Compute $\lambda_n = \langle \hat{\mathbf{U}}_n, \mathbf{H}(\mathbf{U}_n) \hat{\mathbf{U}}_n \rangle$.
- 4: Compute the residual $\mathbf{r}_n = \mathbf{H}(\mathbf{U}_n) \hat{\mathbf{U}}_n - \lambda_n \hat{\mathbf{U}}_n$.
- 5: Compute the relative error $\varepsilon_n = \|\mathbf{r}_n\| / \max\{1, |\lambda_n|\}$.
- 6: **if** $\varepsilon_n < \epsilon$ **then**
- 7: proceed to step 14.
- 8: **end if**
- 9: Apply the preconditioner (4.1) to handle the residual, and obtain the subspace matrix $\mathbf{W}_n = [\hat{\mathbf{U}}_n, \mathbf{p}_n, \mathbf{P}_n \mathbf{r}_n]$.
- 10: Solve the generalized eigenvalue problem $\mu \mathbf{W}_n^T \mathbf{W}_n \mathbf{y} = \mathbf{W}_n^T \mathbf{H}(\mathbf{U}_n) \mathbf{W}_n \mathbf{y}$ for the smallest eigenvalue and its corresponding eigenvector $\mathbf{y}_n = (y_n^{(1)}, y_n^{(2)}, y_n^{(3)})$.
- 11: Compute the Ritz vector: $\hat{\mathbf{U}}_{n+1} = y_n^{(1)} \hat{\mathbf{U}}_n + y_n^{(2)} \mathbf{p}_n + y_n^{(3)} \mathbf{P}_n \mathbf{r}_n$.
- 12: Compute the search direction: $\mathbf{p}_{n+1} = (y_n^{(2)} \mathbf{p}_n + y_n^{(3)} \mathbf{P}_n \mathbf{r}_n) / \|\hat{\mathbf{U}}_{n+1}^-\|_2$.

- 13: Normalize: $\hat{\mathbf{U}}_{n+1} = \hat{\mathbf{U}}_{n+1}^- / \|\hat{\mathbf{U}}_{n+1}^-\|_2$. Proceed to step 3.
 14: Taking $(\lambda_n, \hat{\mathbf{U}}_n)$ as the numerical solution for the smallest eigenpair of (2.7), we then compute the approximate value of the ground state energy $E_K(\hat{\mathbf{U}}_n)$ using (2.9).
 15: **end for**
-

Next, we discuss the computational cost of Algorithm 4.1. First, for nonlinear problems, a quantitative convergence estimate of the locally optimal preconditioned conjugate gradient iteration for nonlinear problems remains an unsolved challenge. Therefore, for the iteration of Algorithm 4.1, we can only provide an estimate of computational cost per iteration step. The asymptotic time complexity of discrete sine transform and its inverse transform is of order $\mathcal{O}(K^d \log K)$, which is slightly higher than the order $\mathcal{O}(K^d)$ of other vector operations (such as addition, scalar multiplication, left-multiplication by a diagonal matrix, etc). However, the discrete sine transform and its inverse are only used when computing the action of the linear operator $\mathbf{H}(\mathbf{U}_n)$ on a vector. Therefore, we may as well use the number of computations of the linear operator to measure the computational cost per iteration. Note that the vector $\mathbf{H}(\mathbf{U}_n)\hat{\mathbf{U}}_n$ is used in computing the eigenvalue (step 3), the residual (step 4), and the elements of the third-order matrix (step 10). Instead of computing it separately for each step, we should compute this vector only once to fulfill the requirements of all three steps. Similarly, $\mathbf{H}(\mathbf{U}_n)\mathbf{p}_n$ and $\mathbf{H}(\mathbf{U}_n)\mathbf{P}_n\mathbf{r}_n$ also need to be computed only once per iteration. This implies that a total of three linear operator computations are required in each iteration.

The locally optimal preconditioned conjugate gradient method employs the Rayleigh-Ritz projection to obtain the optimal search direction, whereas the discrete gradient flow method implicitly determines the search direction. From a practical perspective, the locally optimal PCG method offers two main advantages over the discrete gradient flow method. First, it does not require a time step to limit the search range and can quickly reach the vicinity of the ground state. Second, it avoids solving systems of linear algebraic equations in each iteration, significantly reducing the computational cost per iteration step. The disadvantage of locally optimal preconditioned conjugate gradient method is that it does not have energy diminishing like discrete gradient flow method, which leads to its lack of effective stability theory. In fact, both algorithms lack quantitative estimates of their convergence rates. Consequently, the computational efficiency of these two methods can ultimately only be judged through numerical experiments.

5. Numerical experiments

In this section, we present the numerical results obtained through the discrete gradient flow method and the locally optimal preconditioned conjugate gradient method. All simulations of this section are accomplished with C++ programming language (Microsoft Visual Studio 2022 development environment), and run on the computer with an Intel (R) Core (TM) i7-12700 CPU and 16.00 GB of RAM.

In the numerical experiments of this section, we uniformly employ the threshold $\epsilon = 10^{-8}$. The initial function for iteration is selected as $(2/R)^{d/2} \prod_{j=1}^d \sin(x_j \pi/R)$. Additionally, when using the discrete gradient flow method, unless otherwise specified, we set the time step size to $\Delta t = 0.1$.

Example 5.1. Consider the one dimensional space-fractional nonlinear Schrödinger equation (1.6) with domain $\Omega = (0, R)$ with $R = 100$. The potential energy function is selected as the hat potential

$$V(x) = \left| x - \frac{R}{2} \right|, \quad (5.1)$$

and the functional form of the nonlinear term is

$$f(s) = s. \quad (5.2)$$

This example considers a defocusing nonlinear term. Fig. 1 presents the function images of the ground state solution when the derivative order takes different values.

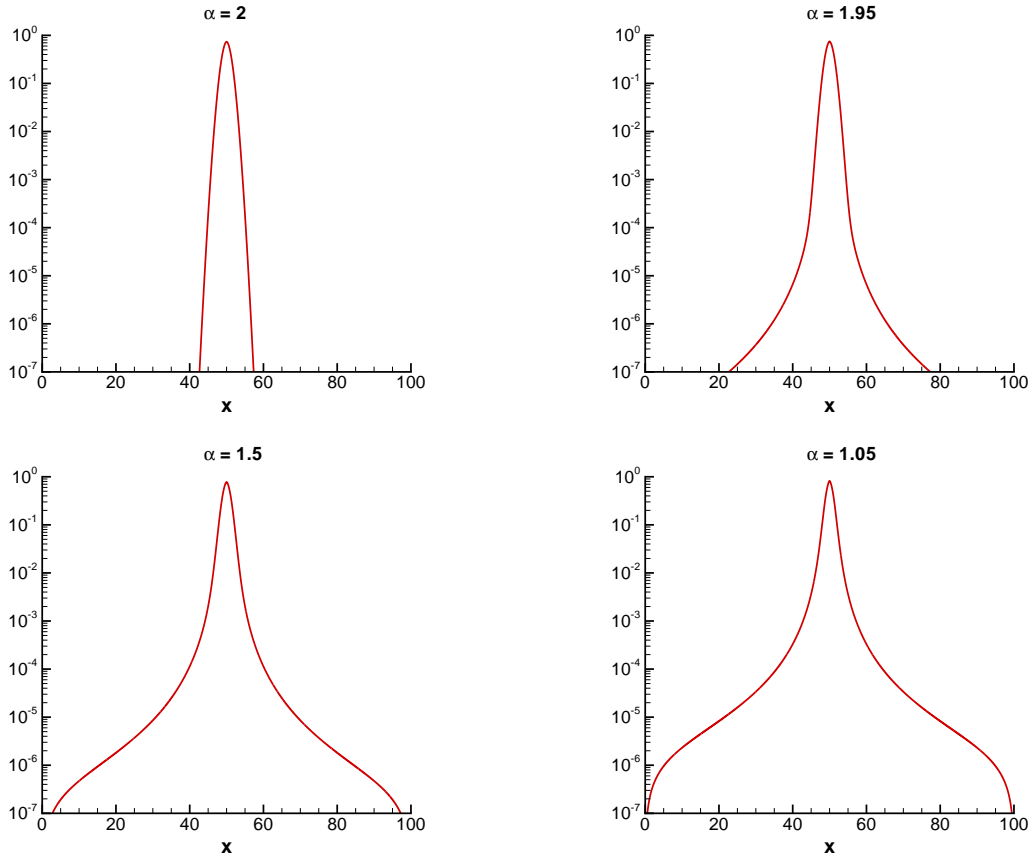


Figure 1: Numerical solutions for Example 5.1.

In the integer-order case ($\alpha = 2$), the solution can quickly approach to zero in a finite. In contrast, in the fractional-order case, especially when the derivative order is small, the decay rate of the solution is significantly weaker. This implies that in order to fit existing physical problems with higher accuracy, fractional-order cases may require a larger region. Tables 1 and 2 present the computational errors of the ground state energy and the eigenfunctions (using the numerical result of $K = 2^{18}$ as the reference solution). Due to the non-smooth potential function affecting the regularity of the solution, the sine pseudospectral method fails to achieve spectral accuracy, attaining only approximately second-order convergence accuracy.

Tables 3 and 4 present the iteration counts for the discrete gradient flow method and the locally optimal preconditioned conjugate gradient method, respectively. In most cases, the locally optimal preconditioned conjugate gradient method requires significantly fewer iterations than the discrete gradient flow method. However, the preconditioner's ability to mitigate the matrix condition number is limited. When parameter K becomes excessively large, the preconditioned matrix remains ill-conditioned, ultimately leading to a substantial increase in iteration counts for the locally optimal preconditioned conjugate gradient method. Nevertheless, since the condition number

Table 1: Energy computational error for Example 5.1.

K	$\alpha = 2$	$\alpha = 1.95$	$\alpha = 1.5$	$\alpha = 1.05$
2^8	1.418E-02	1.430E-02	1.571E-02	1.770E-02
2^{10}	8.649E-04	8.722E-04	9.524E-04	1.071E-03
2^{12}	5.396E-05	5.441E-05	5.935E-05	6.660E-05
2^{14}	3.360E-06	3.388E-06	3.695E-06	4.145E-06
2^{16}	1.976E-07	1.993E-07	2.174E-07	2.438E-07

Table 2: L^2 -error of eigenfunction for Example 5.1.

K	$\alpha = 2$	$\alpha = 1.95$	$\alpha = 1.5$	$\alpha = 1.05$
2^8	8.336E-04	8.613E-04	1.213E-03	1.846E-03
2^{10}	4.906E-05	5.059E-05	7.038E-05	1.149E-04
2^{12}	3.053E-06	3.146E-06	4.351E-06	7.074E-06
2^{14}	1.900E-07	1.959E-07	2.707E-07	4.383E-07
2^{16}	1.118E-08	1.152E-08	1.592E-08	2.577E-08

Table 3: Iteration steps of the discrete gradient flow method for Example 5.1.

K	$\alpha = 2$	$\alpha = 1.95$	$\alpha = 1.5$	$\alpha = 1.05$
2^8	130	130	141	160
2^{10}	130	131	142	160
2^{12}	130	131	142	160
2^{14}	130	131	142	160
2^{16}	130	131	142	160

of the original matrix is approximately proportional to K^α , when the derivative order α is relatively small (close to 1), even at $K = 2^{16}$, the preconditioner effectively controls the matrix condition number. Consequently, the iteration count of the locally optimal preconditioned conjugate gradient method shows no significant increase. This demonstrates that the locally optimal preconditioned conjugate gradient method is better suited for fractional-order problems with lower derivative orders.

Tables 5 and 6 present the time cost for the discrete gradient flow method and the locally optimal preconditioned conjugate gradient method, respectively. Since each iteration of the discrete gradient flow method requires solving an algebraic system, the computational cost per iteration is substantially higher compared to the locally optimal preconditioned conjugate gradient method. In most cases, the time cost of the locally optimal preconditioned conjugate gradient method ranges between 1/30 and 1/10 of that required by the discrete gradient flow method. Even under unfavorable conditions ($\alpha = 2$, $K = 2^{16}$), the time cost of the locally optimal preconditioned conjugate gradient method remains less than a quarter of the discrete gradient flow method's time.

Table 4: Iteration steps of the locally optimal preconditioned conjugate gradient method for Example 5.1.

K	$\alpha = 2$	$\alpha = 1.95$	$\alpha = 1.5$	$\alpha = 1.05$
2^8	57	58	61	62
2^{10}	57	58	61	62
2^{12}	87	83	61	63
2^{14}	189	173	86	63
2^{16}	415	375	149	65

Table 5: Time cost (in seconds) for testing Example 5.1 through the discrete gradient flow method.

K	$\alpha = 2$	$\alpha = 1.95$	$\alpha = 1.5$	$\alpha = 1.05$
2^8	0.04	0.04	0.05	0.05
2^{10}	0.14	0.15	0.16	0.20
2^{12}	0.94	0.96	1.06	1.17
2^{14}	4.23	4.36	4.60	5.18
2^{16}	30.28	29.51	33.19	37.49

Table 6: Time cost (in seconds) for testing Example 5.1 through the locally optimal preconditioned conjugate gradient method.

K	$\alpha = 2$	$\alpha = 1.95$	$\alpha = 1.5$	$\alpha = 1.05$
2^8	-	-	-	-
2^{10}	0.01	0.01	0.01	0.01
2^{12}	0.05	0.05	0.04	0.04
2^{14}	0.48	0.44	0.22	0.16
2^{16}	6.42	5.83	2.30	1.10

Example 5.2. Consider the one dimensional space-fractional nonlinear Schrödinger equation (1.6) with domain $\Omega = (0, R)$, with $R = 100$. Furthermore, the potential function is still taken as (5.1), and we adopt the following saturated nonlinear term:

$$f(s) = \frac{-100s}{1+s}. \quad (5.3)$$

In this example, we consider the focusing saturated nonlinear term, which is negative and bounded for $s \geq 0$. From Fig. 2, it can be seen that the ground state solution function exhibits a sharper shape at the midpoint, and this is caused by the focusing nonlinearity. Furthermore, in this example, when using the simple iterative (3.4), the vector $\mathbf{f}(\mathbf{U}_n)$ has a very large maximum modulus, which makes the format more prone to divergence. Therefore, when using the discrete gradient flow, it is necessary to reduce the time step Δt to ensure that the iteration calculation of the algebraic equations converges.

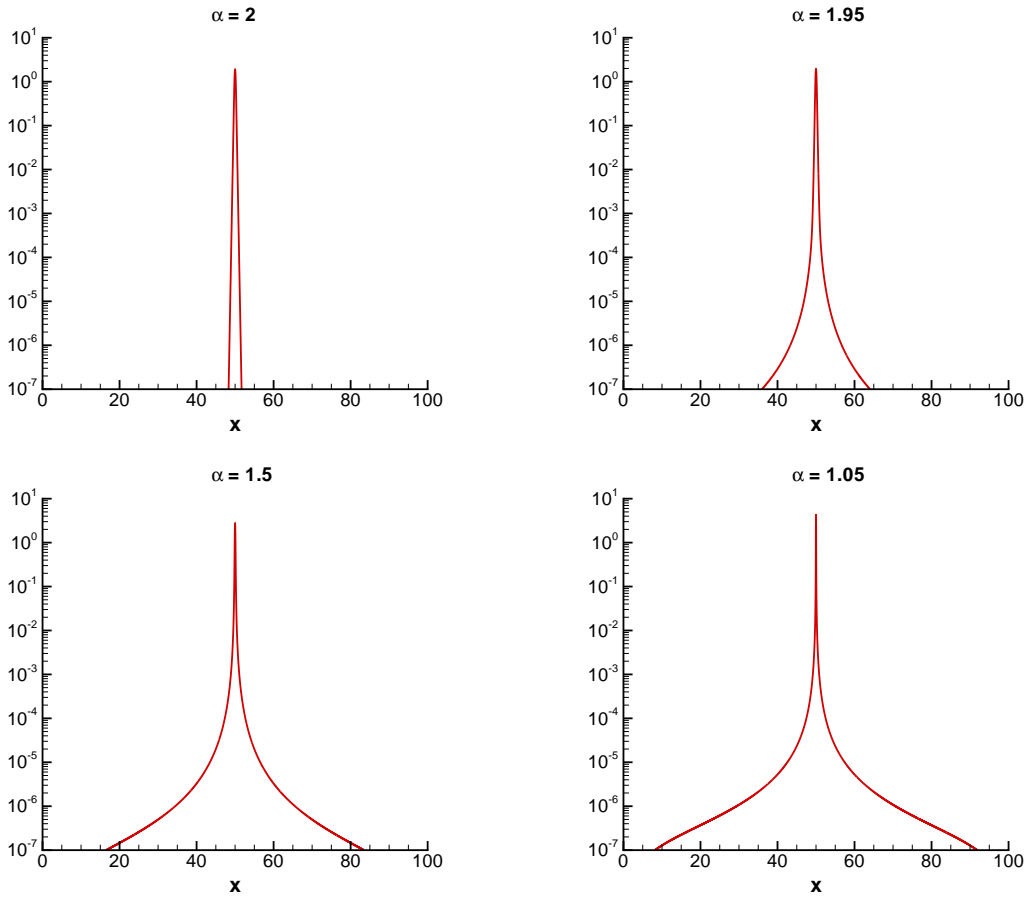


Figure 2: Numerical solutions for Example 5.2.

Tables 7 and 9 indicate that the convergence rate of the discrete gradient flow method actually becomes faster than previous example. This may be due to the localization of the solution function has become stronger, which leads to a clearer decay path of the energy functional, which leads to a clearer decay path for the discrete gradient flow method tend to the minimum energy functional. For the locally optimal preconditioned conjugate gradient method, when the parameter K is relatively small,

Table 7: Iteration steps of the discrete gradient flow method for Example 5.2 ($\Delta t = 0.01$).

K	$\alpha = 2$	$\alpha = 1.95$	$\alpha = 1.5$	$\alpha = 1.05$
2^8	39	38	35	33
2^{10}	57	57	93	33
2^{12}	57	57	62	66
2^{14}	57	57	62	79
2^{16}	57	57	62	79

Table 8: Iteration steps of the locally optimal preconditioned conjugate gradient method for Example 5.2.

K	$\alpha = 2$	$\alpha = 1.95$	$\alpha = 1.5$	$\alpha = 1.05$
2^8	20	19	17	17
2^{10}	50	51	63	19
2^{12}	61	60	52	74
2^{14}	186	154	57	88
2^{16}	662	560	98	88

Table 9: Time cost (in seconds) for testing Example 5.2 through the discrete gradient flow method ($\Delta t = 0.01$).

K	$\alpha = 2$	$\alpha = 1.95$	$\alpha = 1.5$	$\alpha = 1.05$
2^8	0.01	0.01	0.01	0.01
2^{10}	0.05	0.05	0.10	0.04
2^{12}	0.26	0.26	0.37	0.61
2^{14}	1.23	1.21	1.76	3.45
2^{16}	8.22	8.41	12.64	24.83

Table 10: Time cost (in seconds) for testing Example 5.2 through the locally optimal preconditioned conjugate gradient method.

K	$\alpha = 2$	$\alpha = 1.95$	$\alpha = 1.5$	$\alpha = 1.05$
2^8	-	-	-	-
2^{10}	0.01	0.01	0.01	-
2^{12}	0.03	0.03	0.03	0.04
2^{14}	0.41	0.34	0.13	0.19
2^{16}	8.95	7.99	1.50	1.38

it also converges faster due to the stronger localization. However, when K is large and the derivative-order is closed to 2, Tables 8 and 10 show that the iteration steps of locally optimal preconditioned conjugate gradient method have significantly increased. This is because in discrete scheme (2.7), both the action of fractional Laplacian Λ and the action of potential $\mathbf{S}\mathbf{V}\mathbf{S}^{-1} + \mathbf{S}\mathbf{f}(\mathbf{U})\mathbf{S}^{-1}$ exhibit strong ill-conditioned. And this dual ill-conditioned matrices will reduce the effect of the preconditioner, resulting in slower the convergence of locally optimal preconditioned conjugate gradient method. But when the derivative order is lower, this negative effect is significantly weaker.

Example 5.3. Consider the multi dimensional space-fractional nonlinear Schrödinger equation (1.6) with domain $\Omega = (0, R)^d$ with $R = 40$. Furthermore, the potential function is taken to be of the multi-dimensional harmonic oscillator type

$$V(\mathbf{x}) = \frac{1}{2} \sum_{j=1}^d \left(x_j - \frac{R}{2} \right)^2, \quad (5.4)$$

and the nonlinear interaction function is the same to (5.2).

In this example, we consider a multidimensional case where the potential function is replaced with a harmonic oscillator potential. Fig. 3 displays numerical results

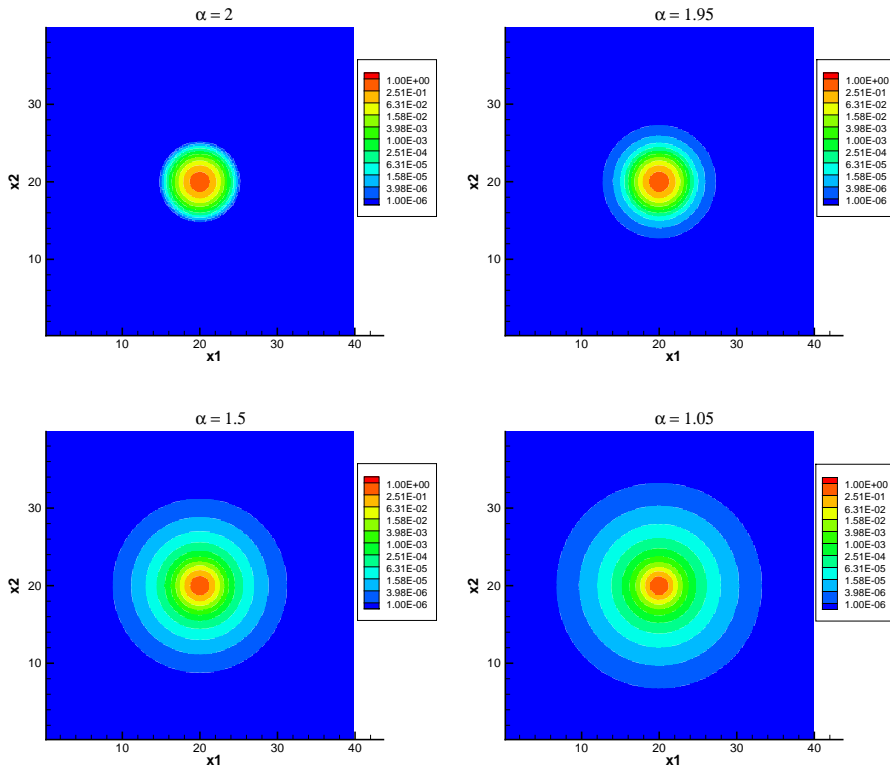


Figure 3: Numerical solutions for Example 5.3 in two-dimensional case.

for two-dimensional case. The main distribution region of the ground state solution significantly expands as the order of the derivative decreases, consequently leading to weaker decay characteristics. From Tables 11-14, it can be observed that the sine pseudo-spectral method achieves computational convergence comparable to spectral accuracy, since the potential function adopted in this example is smooth. However, when the derivative order is low, the computational effectiveness of spectral accuracy diminishes. This occurs because, in the fractional-order case, the solution function exhibits slower decay. This property creates a minor conflict with the homogeneous Dirichlet boundary conditions, reducing the regularity of the solution function near the boundaries. Ultimately, this impacts the spectral accuracy convergence performance of the sine pseudo-spectral method.

Table 11: Energy computational error for Example 5.3 in two dimensions.

K	$\alpha = 2$	$\alpha = 1.95$	$\alpha = 1.5$	$\alpha = 1.05$
2^4	5.067E-01	5.035E-01	4.798E-01	4.462E-01
2^5	6.002E-04	3.912E-04	3.005E-03	1.018E-02
2^6	4.698E-07	6.193E-07	7.053E-06	7.079E-05
2^7	<1E-08	<1E-08	<1E-08	<1E-08

Table 12: L^2 -error of eigenfunction for Example 5.3 in two dimensions.

K	$\alpha = 2$	$\alpha = 1.95$	$\alpha = 1.5$	$\alpha = 1.05$
2^4	2.073E-02	2.095E-02	2.321E-02	2.628E-02
2^5	1.282E-03	1.382E-03	2.603E-03	4.605E-03
2^6	4.575E-06	5.590E-06	3.364E-05	1.884E-04
2^7	<1E-08	<1E-08	<1E-08	2.065E-07

Table 13: Energy computational error for Example 5.3 in three dimensions.

K	$\alpha = 2$	$\alpha = 1.95$	$\alpha = 1.5$	$\alpha = 1.05$
2^4	7.615E-01	7.576E-01	7.082E-01	6.305E-01
2^5	8.283E-03	9.385E-03	2.500E-02	5.229E-02
2^6	1.598E-07	2.101E-07	2.127E-06	1.830E-05
2^7	<1E-08	<1E-08	<1E-08	<1E-08

Table 14: L^2 -error of eigenfunction for Example 5.3 in three dimensions.

K	$\alpha = 2$	$\alpha = 1.95$	$\alpha = 1.5$	$\alpha = 1.05$
2^4	5.759E-03	5.835E-03	6.647E-03	7.736E-03
2^5	5.016E-04	5.446E-04	1.085E-03	1.965E-03
2^6	8.734E-07	1.099E-06	8.503E-06	5.914E-05
2^7	<1E-08	<1E-08	<1E-08	4.927E-08

Tables 15 and 16 present the iteration steps of two algorithms for solving two-dimensional problem. In this case, the degree of localization of the ground state solution is the primary factor influencing the convergence speed of the numerical iterative methods. Consequently, when the derivative order α is relatively low, the iteration steps increase for both algorithms, with the discrete gradient flow method being more significantly affected in contrast. Unlike the previous examples, the selected values of K in this case are not excessively large. Under the action of preconditioners, issues related to ill-conditioned matrices did not arise. Therefore, the condition number did not become a major factor affecting the convergence speed of the locally optimal preconditioned conjugate gradient method. Tables 15 and 18 show the time cost of two algorithms in two-dimensional case. Because the number of iterations required for solving the algebraic system (3.4) in this example increases markedly compared with the previous cases, the discrete gradient flow method takes considerably longer to compute than the locally optimal preconditioned conjugate gradient method. This gap becomes even more pronounced in the three-dimensional case: in Tables 19 and 20 one can see that the difference in computational efficiency between two algorithms reaches roughly a factor of 100, and the lower the fractional derivative order, the larger the efficiency disparity. Overall, the locally optimal preconditioned conjugate gradient method enjoys a more prominent efficiency advantage in multidimensional problems than in the one-dimensional case.

Table 15: Iteration steps of the discrete gradient flow method for Example 5.3 in two-dimensional case.

K	$\alpha = 2$	$\alpha = 1.95$	$\alpha = 1.5$	$\alpha = 1.05$
2^4	80	80	81	82
2^5	113	116	143	188
2^6	110	112	135	172
2^7	110	112	135	171

Table 16: Iteration steps of the locally optimal preconditioned conjugate gradient method for Example 5.3 in two-dimensional case.

K	$\alpha = 2$	$\alpha = 1.95$	$\alpha = 1.5$	$\alpha = 1.05$
2^4	120	120	125	125
2^5	164	165	182	202
2^6	165	166	181	205
2^7	165	167	180	201

Table 17: Time cost (in seconds) for testing Example 5.3 in two-dimensional case through the discrete gradient flow method.

K	$\alpha = 2$	$\alpha = 1.95$	$\alpha = 1.5$	$\alpha = 1.05$
2^4	0.21	0.21	0.22	0.24
2^5	1.07	1.11	1.38	1.80
2^6	4.81	4.87	5.86	7.35
2^7	16.53	17.30	20.15	26.56

Table 18: Time cost (in seconds) for testing Example 5.3 in two-dimensional case through the locally optimal preconditioned conjugate gradient method.

K	$\alpha = 2$	$\alpha = 1.95$	$\alpha = 1.5$	$\alpha = 1.05$
2^4	0.01	0.01	0.01	0.01
2^5	0.03	0.03	0.03	0.04
2^6	0.10	0.11	0.12	0.13
2^7	0.32	0.33	0.35	0.39

Table 19: Time cost (in seconds) for testing Example 5.3 in the three-dimensional case through the discrete gradient flow method.

K	$\alpha = 2$	$\alpha = 1.95$	$\alpha = 1.5$	$\alpha = 1.05$
2^4	23.78	23.65	27.71	33.81
2^5	65.57	66.56	72.85	84.22
2^6	677.93	677.55	834.74	1205.25
2^7	5298.37	5274.73	6595.15	9096.81

Table 20: Time cost (in seconds) for testing Example 5.3 in the three-dimensional case through the locally optimal preconditioned conjugate gradient method.

K	$\alpha = 2$	$\alpha = 1.95$	$\alpha = 1.5$	$\alpha = 1.05$
2^4	0.15	0.15	0.15	0.15
2^5	1.07	1.07	1.27	1.46
2^6	8.70	8.87	10.19	11.66
2^7	67.85	65.91	75.32	87.92

Example 5.4. Consider the two dimensional space-fractional nonlinear Schrödinger equation (1.6) with domain $\Omega = (0, R)^d$ with $R = 40$. Furthermore, adopt the potential function (5.4) and the nonlinear interaction function

$$f(s) = -s.$$

This example considers a two-dimensional focusing nonlinear problem. Fig. 4 presents ground state solutions for case $\alpha = 2, 1.95$ and 1.5 . When α is taken as 1.05 , Fig. 5 shows that the numerical solution becomes highly concentrated at the center point, and the supremum of the function is determined by the parameter K . This numerical result implies that the quantum state has collapsed. Furthermore, in the nonlinear scenario, Table 21 shows that the energy functional of the collapsed state is tend to negative infinity with the increase of K .

For cases where classical solutions exist ($\alpha = 2, 1.95, 1.5$), Tables 22-25 present the computational performance of two numerical iterative methods. The comparative outcomes are similar to those in Example 5.3. In this example, greater attention is given to the comparison of numerical performance under energy collapse conditions ($\alpha = 1.05$). Relevant results are shown in Tables 26 and 27. When the value of K

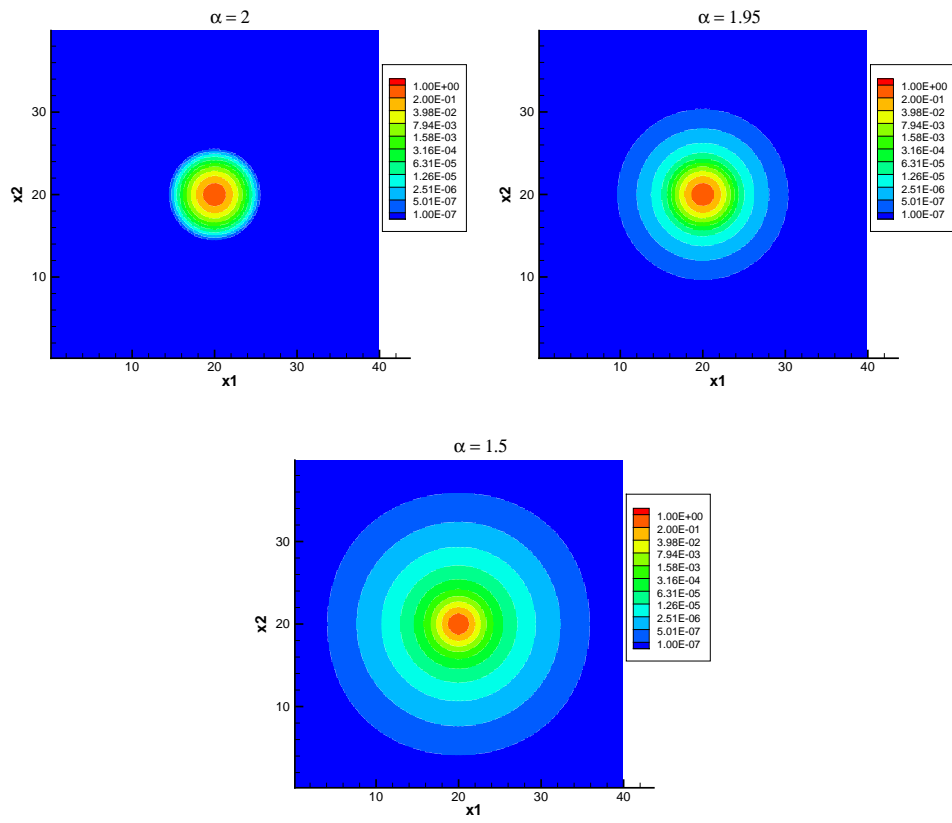


Figure 4: Numerical solution for Example 5.4 under the cases of $\alpha = 2$, 1.95 and 1.5.

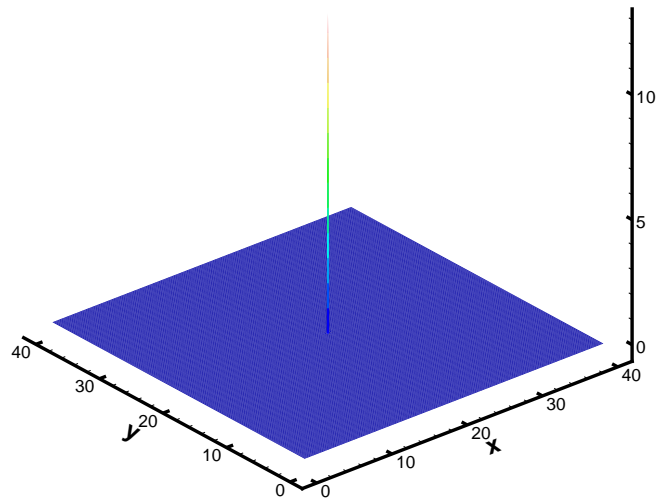


Figure 5: Numerical solution for Example 5.4 with $\alpha = 1.05$ and $K = 512$.

Table 21: The discrete energy values of Example 5.4 for different values of K when $\alpha = 1.05$.

K	2^5	2^6	2^7	2^8	2^9
Discrete energy	0.5684	0.5146	-1.1287	-11.9198	-63.8964

Table 22: Iteration steps of the discrete gradient flow method for Example 5.4.

K	$\alpha = 2$	$\alpha = 1.95$	$\alpha = 1.5$
2^4	73	73	74
2^5	142	146	176
2^6	120	123	178
2^7	120	123	169

Table 23: Iteration steps of the locally optimal preconditioned conjugate gradient method for Example 5.4.

K	$\alpha = 2$	$\alpha = 1.95$	$\alpha = 1.5$
2^4	119	119	123
2^5	186	189	210
2^6	179	180	207
2^7	181	183	210

Table 24: Time cost (in seconds) for testing Example 5.4 by the discrete gradient flow method.

K	$\alpha = 2$	$\alpha = 1.95$	$\alpha = 1.5$
2^4	0.19	0.19	0.21
2^5	1.40	1.42	1.88
2^6	5.96	5.37	7.73
2^7	18.12	18.70	25.67

Table 25: Time cost (in seconds) for testing Example 5.4 through the locally optimal preconditioned conjugate gradient method.

K	$\alpha = 2$	$\alpha = 1.95$	$\alpha = 1.5$
2^4	0.01	0.01	0.01
2^5	0.03	0.03	0.04
2^6	0.13	0.13	0.14
2^7	0.37	0.37	0.39

Table 26: Iteration steps and time cost (in seconds) of the discrete gradient flow method for Example 5.4 when $\alpha = 1.05$.

$(K, \Delta t)$	$(2^5, 10^{-1})$	$(2^6, 10^{-1})$	$(2^7, 10^{-1})$	$(2^8, 10^{-2})$	$(2^9, 10^{-3})$
Iteration steps	174	209	95	769	7344
Time cost	1.70	9.72	20.41	85.38	771.37

Table 27: Iteration steps and time cost (in seconds) of the locally optimal preconditioned conjugate gradient method for Example 5.4 when $\alpha = 1.05$.

K	2^5	2^6	2^7	2^8	2^9
Iteration steps	255	378	363	156	112
Time cost	0.05	0.23	0.70	1.45	3.69

is large, the singularity of the numerical solution also increases. Due to the enhanced singularity of the solution function, the discrete gradient flow method must reduce the time step to ensure the iterative convergence of the linear algebraic equations, resulting in a significant increase in the number of discrete gradient flow iterations. In contrast, the efficiency of the locally optimal preconditioned conjugate gradient method is not noticeably affected by the singularity of the numerical solution. From these results, it can be observed that both the discrete gradient flow method and the locally optimal preconditioned conjugate gradient method can effectively address singularity issues. However, in terms of efficiency, the locally optimal preconditioned conjugate gradient method clearly holds an advantage.

6. Conclusion and future work

The primary contribution of this work is the application of locally optimal preconditioned conjugate gradient method to compute the ground state of space-fractional nonlinear Schrödinger equation, with its advantages demonstrated through comparative analysis against the traditional discrete gradient flow method. Numerical results indicate that the locally optimal preconditioned conjugate gradient method outperforms the discrete gradient flow method in many common scenarios, particularly for multidimensional problems and cases involving lower fractional derivative orders. However, when the discrete parameter K or the nonlinear coefficient assumes larger values, the advantage of locally optimal preconditioned conjugate gradient method may be weakened. Both algorithms exhibit robust stability when addressing collapse states, though the locally optimal preconditioned conjugate gradient method demonstrates significantly superior computational efficiency. For future work, we plan to further explore the computation for excited states of space-fractional nonlinear Schrödinger equation. We can combine the idea of locally optimal preconditioned conjugate gradient method with special algorithms for solving excited states such as shift inverse iteration method and J -method [1, 15], to design efficient and stable numerical methods for computing the nonlinear fractional-order excited states.

Acknowledgments

This work is supported by the National Natural Science Foundation of China (Grant No. 12471391), by the Scientific Research Fund of Hunan Provincial Education De-

partment (Grant No. 23A0127) and by the Hunan Provincial Innovation Foundation for Postgraduate (Grant No. CX20230615).

References

- [1] R. ALTMANN, P. HENNING, AND D. PETERSEIM, *The J-method for the Gross-Pitaevskii eigenvalue problem*, Numer. Math. 148 (2021), 575–610.
- [2] X. ANTOINE, A. LEVITT, AND Q. TANG, *Efficient spectral computation of the stationary states of rotating Bose-Einstein condensates by preconditioned nonlinear conjugate gradient methods*, J. Comput. Phys. 343 (2017), 92–109.
- [3] W. BAO AND Y. CAI, *Mathematical theory and numerical methods for Bose-Einstein condensation*, Kinet. Relat. Mod. 6 (2013), 1–135.
- [4] W. BAO, I. CHERN, AND F. Y. LIM, *Efficient and spectrally accurate numerical methods for computing ground and first excited states in Bose-Einstein condensates*, J. Comput. Phys. 219 (2006), 836–854.
- [5] W. BAO AND Q. DU, *Computing the ground state solution of Bose-Einstein condensates by a normalized gradient flow*, SIAM J. Sci. Comput. 25 (2004), 1674–1697.
- [6] P. BENNER AND X. LIANG, *Convergence analysis of vector extended locally optimal block preconditioned extended conjugate gradient method for computing extreme eigenvalues*, Numer. Lin. Alg. Appl. 29 (2022), Paper No. e2445.
- [7] F. D. M. BEZERRA, A. N. CARVALHO, T. DLOTKO, AND M. J. D. NASCIMENTO, *Fractional Schrödinger equation; solvability and connection with classical Schrödinger equation*, J. Math. Anal. Appl. 457 (2018), 336–360.
- [8] Y. CAI AND W. LIU, *Efficient and accurate gradient flow methods for computing ground states of spinor Bose-Einstein condensates*, J. Comput. Phys. 433 (2021), Paper No. 110183.
- [9] X. CHANG, *Ground state solutions of asymptotically linear fractional Schrödinger equations*, J. Math. Phys. 54 (2013), Paper No. 061504.
- [10] C. A. DARTORA, F. ZANELLA, AND G. G. CABRERA, *Emergence of fractional quantum mechanics in condensed matter physics*, Phys. Lett. A 415 (2021), Paper No. 127643.
- [11] C. DU AND C. LIU, *Newton-Noda iteration for computing the ground states of nonlinear Schrödinger equations*, SIAM J. Sci. Comput. 44 (2022), A2370–A2385.
- [12] S. DUO AND Y. ZHANG, *Computing the ground and first excited states of the fractional Schrödinger equation in an infinite potential well*, Commun. Comput. Phys. 18 (2015), 321–350.
- [13] S. DUO AND Y. ZHANG, *Mass-conservative Fourier spectral methods for solving the fractional nonlinear Schrödinger equation*, Comput. Math. Appl. 71 (2016), 2257–2271.
- [14] M. R. HESTENES AND E. STIEFEL, *Methods of conjugate gradients for solving linear systems*, J. Res. Natl. Bur. Stand. 49 (1952), 409–436.
- [15] E. JARLEBRING, S. KVAAL, AND W. MICHIELS, *An inverse iteration method for eigenvalue problems with eigenvector nonlinearities*, SIAM J. Sci. Comput. 36 (2014), A1978–A2001.
- [16] A. V. KNYAZEV, *A preconditioned conjugate gradient method for eigenvalue problems and its implementation in a subspace*, Internat. Series Numer. Math. 96 (1991), 143–154.
- [17] A. V. KNYAZEV, *Toward the optimal preconditioned eigensolver: Locally optimal block preconditioned conjugate gradient method*, SIAM J. Sci. Comput. 23 (2001), 517–541.
- [18] N. LASKIN, *Fractional quantum mechanics and Lévy path integrals*, Phys. Lett. A 268 (2000), 298–305.
- [19] N. LASKIN, *Fractional Schrödinger equation*, Phys. Rev. E 66 (2002), Paper No. 056108.

- [20] M. LI, X. GU, C. HUANG, M. FEI, AND G. ZHANG, *A fast linearized conservative finite element method for the strongly coupled nonlinear fractional Schrödinger equations*, J. Comput. Phys. 358 (2018), 256–282.
- [21] X. LIANG AND Q. M. ABDUL, *An efficient Fourier spectral exponential time differencing method for the space-fractional nonlinear Schrödinger equations*, Comput. Math. Appl. 75 (2018), 4438–4457.
- [22] L. LIU AND K. TENG, *Ground state and multiple solutions for critical fractional Schrödinger-poisson equations with perturbation terms*, Electron. J. Differ. Eq. 2021 (2021), 1–21.
- [23] S. LONGHI, *Fractional Schrödinger equation in optics*, Opt. Lett. 40 (2015), 1117–1120.
- [24] C. POZRIKIDIS, *The Fractional Laplacian*, CRC, (2016).
- [25] M. RAN AND C. ZHANG, *A conservative difference scheme for solving the strongly coupled nonlinear fractional Schrödinger equations*, Commun. Nonlinear Sci. Numer. Simul. 41 (2016), 64–83.
- [26] C. SULEM AND P. L. SULEM, *The Nonlinear Schrödinger Equation: Self-Focusing and Wave Collapse*, Springer-Verlag, (1999).
- [27] D. WANG, A. XIAO, AND W. YANG, *A linearly implicit conservative difference scheme for the space fractional coupled nonlinear Schrödinger equations*, J. Comput. Phys. 272 (2014), 644–655.
- [28] P. WANG AND C. HUANG, *A conservative linearized difference scheme for the nonlinear fractional Schrödinger equation*, Numer. Algor. 69 (2015), 625–641.
- [29] M. I. WEINSTEIN, *Nonlinear Schrödinger equations and sharp interpolation estimates*, Comm. Math. Phys. 87 (1983), 567–576.
- [30] H. YANG, *Conjugate gradient method for the Rayleigh quotient minimization of generalized eigenvalue problems*, Computing 51 (1993), 79–94.
- [31] Y. YANG, X. LI, AND A. XIAO, *Fourier pseudospectral method for fractional stationary Schrödinger equation*, Appl. Numer. Math. 165 (2021), 137–151.
- [32] Y.-Q. ZHANG, H. ZHONG, M. BELIĆ, N. AHMED, Y.-P. ZHANG, AND M. XIAO, *Diffraction-free beams in fractional Schrödinger equation*, Sci. Rep. 6 (2016), Paper No. 23645.
- [33] X. ZHAO, Z. SUN, AND Z. HAO, *A fourth-order compact ADI scheme for two-dimensional nonlinear space fractional Schrödinger equation*, SIAM J. Sci. Comput. 36 (2014), A2865–A2886.